Journal of Nano- and Electronic Physics
Vol. **11** No 4, 04005(5pp) (2019)

Журнал нано- та електронної фізики
Том **11** № 4, 04005(5cc) (2019)

Electrical Characteristics of Au/*n*-GaN Schottky Junction with a High-*k* $SrTiO_3$ Insulating Layer

Varra Niteesh Reddy, D.V. Vivekananda, G. Sai Krishna, B. Sri Vivek, P. Vimala*

Department of Electronics & Communication Engineering, Dayananda Sagar College of Engineering, Shavige Malleshwara Hills, Kumaraswamy Layout, Banashankari, Bengaluru-560078, Karnataka, India

(Received 07 May 2019; revised manuscript received 01 August 2019; published online 22 August 2019)

The electrical characteristics of Au/*n*-GaN Schottky junction (SJ) were improved by a place of high-*k* strontium titanate ($SrTiO_3$) insulating layer in the middle of Au and n-GaN. The electrical properties of Au/*n*-GaN SJ and Au/$SrTiO_3$/n-GaN metal/insulator/semiconductor (MIS) junction were explored by current-voltage and capacitance-voltage techniques. The MIS junction displayed an exquisite rectifying nature as compared to the SJ. The series resistance (R_S) and shunt resistance (R_{Sh}) were found to be 30 Ω, 4.69×10^6 Ω and 250 Ω, 2.12×10^9 Ω for the SJ and MIS junction, respectively. The estimated barrier height (BH) and ideality factors of SJ and MIS junction were 0.67 eV, 1.44 and 0.83 eV, 1.78, respectively. Higher BH was achieved for the MIS junction than the SJ junction, suggesting the BH was effectually changed by the $SrTiO_3$ layer. Also, the ideality factor, BH and series resistance of the SJ and MIS junction were estimated by employing the Cheung's function and compared each other. Observations reveal the ohmic behavior at lower voltage regions and space-charge-limited conduction at higher voltage regions in the forward bias I-V characteristic of the SJ and MIS junctions. Also, the reverse leakage current conduction mechanism of SJ and MIS junctions was explored.

Keywords: *n*-type GaN, Strontium titanate, Electrical properties, MIS junction, Barrier height, Ideality factor, Current conduction mechanism.

DOI: 10.21272/jnep.11(4).04005 PACS numbers: 73.40.Qv, 85.30.Hi

1. INTRODUCTION

III-V wide bandgap semiconductors, mainly gallium nitride (GaN), are essential semiconductor materials for the development of metal/oxide/semiconductor field effect transistors, heterojunction field effect transistors, metal/insulator/semiconductor field effect transistors, high electron mobility transistors, and Schottky rectifiers [1, 2] because of their unique properties. However, Schottky junctions in GaN-based devices suffer from strange leakage current and lower breakdown voltage that limits the device concert and steadfastness. Henceforth, it is imperious to realize good Schottky junctions with a low ideality factor, low leakage current and high barrier height by applying thin insulating/interlayer. Consequently, the complete investigation of fabrication and electrical characteristics of metal/insulator/semiconductor interface is crucial. Different research groups have concentrated on the creation of thin oxide/insulating or interlayer in the middle of the metal and n-type GaN semiconductor, and investigated its electrical characteristics using different approaches [3].

This work primarily emphases on the introduction of high-*k* strontium titanate ($SrTiO_3$) as an insulating layer between the metal and the semiconductor, and tested its outcome on the electrical properties of Au/n-GaN SJ. To achieve superior ultra-large-scale integration (ULSIs) with high recital and low-power consumption, high-*k* materials have fascinated large interest for future gate dielectrics. Therefore, $SrTiO_3$ is chosen as an insulator layer in the present work because it has high dielectric constant, small dielectric loss, large relative permittivity, high breakdown potency, and extremely good thermal strength [4]. Moreover, $SrTiO_3$ is one probable material that may be placed to use for tunable microwave device applications owing to its high dielectric nonlinearity and low dissipation factor [5]. So, the current work is devoted to the development of Au/$SrTiO_3$/*n*-GaN MIS junction with a high-*k* $SrTiO_3$ as an insulating layer and investigates its electrical characteristics. The electronic parameters of Au/$SrTiO_3$/*n*-GaN MIS junction were estimated by current-voltage (I-V) and capacitance-voltage (C-V) measurements. These parameters were compared with that of the conventional Au/n-GaN SJ. As well, the possible forward and reverse current conduction mechanisms of the Au/*n*-GaN SJ and Au/$SrTiO_3$/*n*-GaN MIS junction were described and explained.

2. EXPERIMENTAL DETAILS

Si-doped GaN films (2 μm thick) were employed for the fabrication of Au/($SrTiO_3$)/*n*-GaN metal/insulator/semiconductor (MIS) junction. The growing *n*-GaN films, cleaning process and fabrication methods were followed as stated in [3]. The schematic configuration of a fabricated Au/$SrTiO_3$/*n*-GaN MIS junction is shown in Fig. 1a. To correlate the electrical properties of the Au/$SrTiO_3$/*n*-GaN MIS junction, the Au/n-GaN Schottky junction (SJ) was also prepared on the same GaN substrate as a reference junction. Using a Keithley source measurement unit (Model No: 2400) and automated deep level transient spectrometer (DLS-83D), the electrical properties of the Au/$SrTiO_3$/n-GaN MIS junction and Au/*n*-GaN SJ were measured in the dark, respectively.

* drvimala-ece@dayanandasagar.edu

3. RESULTS AND DISCUSSION

Fig. 1b displays the I-V curves of the SJ and MIS junction measured at room temperature. The SJ and MIS junction exhibit a good rectifying nature (Fig. 1b). The reverse leakage currents of SJ and MIS junction are measured to be 1.8×10^{-6} and 9.5×10^{-8} A at – 1 V, respectively. The MIS junction exhibits a lower reverse leakage current than the SJ, thus indicating that the electrical properties of MIS junction are improved. This is due to the place of high-k $SrTiO_3$ thin insulating layer between the Au and n-GaN layers.

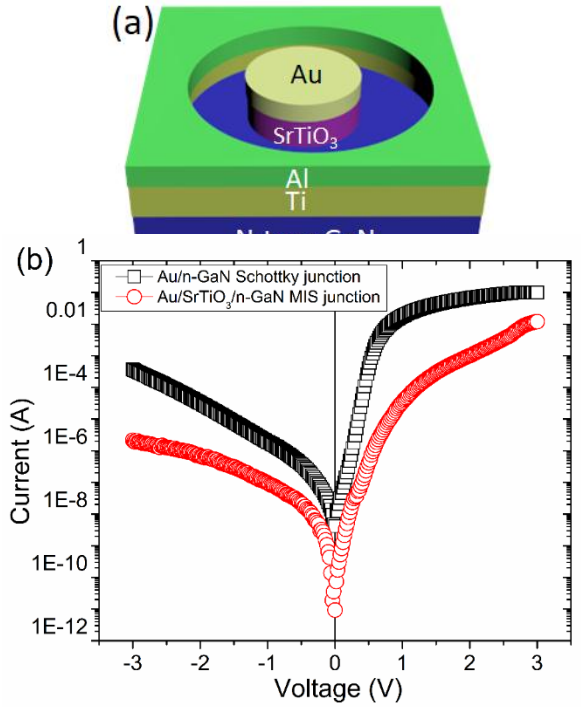

Fig. 1 – Schematic diagram of Au/$SrTiO_3$/n-GaN MIS junction (a), I-V characteristics of Au/n-GaN SJ and Au/$SrTiO_3$/n-GaN MIS junction (b)

The barrier height (BH) and ideality factor of Au/n-GaN SJ and Au/$SrTiO_3$/n-GaN MIS junction are derived. The reverse saturation current of the Au/n-GaN SJ and Au/$SrTiO_3$/n-GaN MIS junction was obtained from the plot of $I/[1 - \exp(-qV/kT)]$ versus voltage (plot not shown here). The BHs of the SJ and MIS junction are found to be 0.67 eV and 0.83 eV, respectively. The estimated BH of MIS junction is greater than the SJ, implying that the BH can be modified by $SrTiO_3$ interlayer. Both junctions showed that BH rises in forward-bias which may be because of the enhance in quasi-Fermi level of the majority carriers on the GaN surface. Thus, the majority of the electrons to be injected directly into the metal which makes a thermionic current through a few electrons are trapped by interface states. As a result, the BH rises thus decreasing the junction current [3]. The ideality factor of SJ and MIS junction are evaluated from the slope of the ln I-V plot. The evaluated ideality factor values of SJ and MIS junction are 1.44 and 1.78, respectively. The SJ and MIS junction show that the determined ideality factor values are more than one. The reasons may be due to (1) barrier inhomogeneity, (2) recombination-generation, (3) image-force effect, (4) tunneling effect and (5) voltage drop present at the insulating layer [6, 7]. Another possibility may be the inhomogeneous BH for greater values of ideality factor. The creation of an electric dipole layer at $SrTiO_3$/n-GaN interface may be accountable for the departure of the ideality factor from unity [8].

In order to estimate the device consistency and effectiveness, the series resistance (R_S) and shunt resistance (R_{Sh}) of the junction play an important role. The values of R_S and R_{Sh} can be determined from the plots of junction resistance ($R_j = \partial V/\partial I$) versus bias voltage ($V$) for the SJ and MIS junction as shown in Fig. 2a, b. The calculated R_S of the SJ and MIS junction are 30 Ω and 250 Ω, respectively. The shunt resistance (R_{Sh}) is also derived for the SJ and MIS junction and the corresponding values are 4.69×10^6 Ω and 2.12×10^9 Ω, respectively. Results indicate that both the SJ and MIS junction have low R_S and high R_{Sh} which are needed for ideal devices.

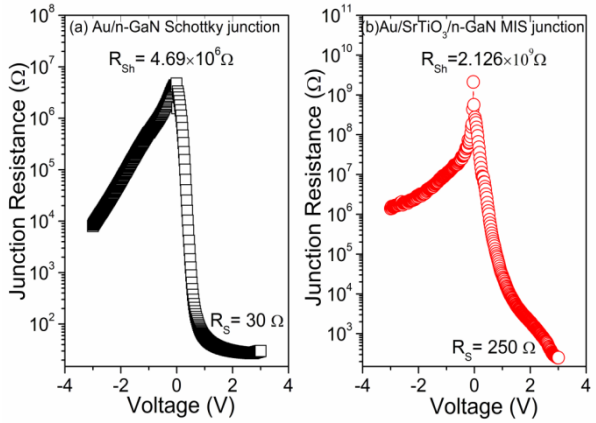

Fig. 2 – Junction resistance (R_j) versus bias voltage for the (a) Au/n-GaN SJ and (b) Au/$SrTiO_3$/n-GaN MIS junction

Furthermore, the Au/n-GaN SJ and Au/$SrTiO_3$/n-GaN MIS junction (Fig. 1b) reveal non-linearity in the forward bias I-V curves at the upper voltage region, which is owing to the effect of series resistance (R_S) and interface state density. To assess the BH, ideality factor and R_S of the SJ and MIS junction in the non-linearity region of I-V curves, Cheung's functions were executed [9]. The $dV/d(\ln I)$-I and $H(I)$-I plots are drawn for the SJ and MIS junction and are depicted in Fig. 3a, b. From $dV/d(\ln I)$-I plot, the ideality factor and series resistance were evaluated as 1.87 and 19 Ω, and 4.16 and 565 Ω for the SJ and MIS junction, respectively. Whereas the R_S and BH are determined to be 18 Ω and 0.61 eV, and 595 Ω and 0.84 eV from $H(I)$-I plot for the SJ and MIS junction, respectively. The R_S values derived from the $dV/d(\ln I)$-I plot are almost comparable to those determined from the $H(I)$-I plot, which confirms that Chenug's functions are reliable and applicable. Results present that the BHs evaluated by $H(I)$-I plot are nearly similar with those derived by the forward-bias $\ln(I)$-V graph. Nevertheless, the ideality factors derived by $dV/d(\ln I)$-I plot are somewhat different from those derived by forward-bias $\ln(I)$-V plot. This may be caused by the effect of both R_S and interfacial layer on the I-V characteristics, although only R_S effects the $dV/d(\ln I)$-I plot [9, 10].

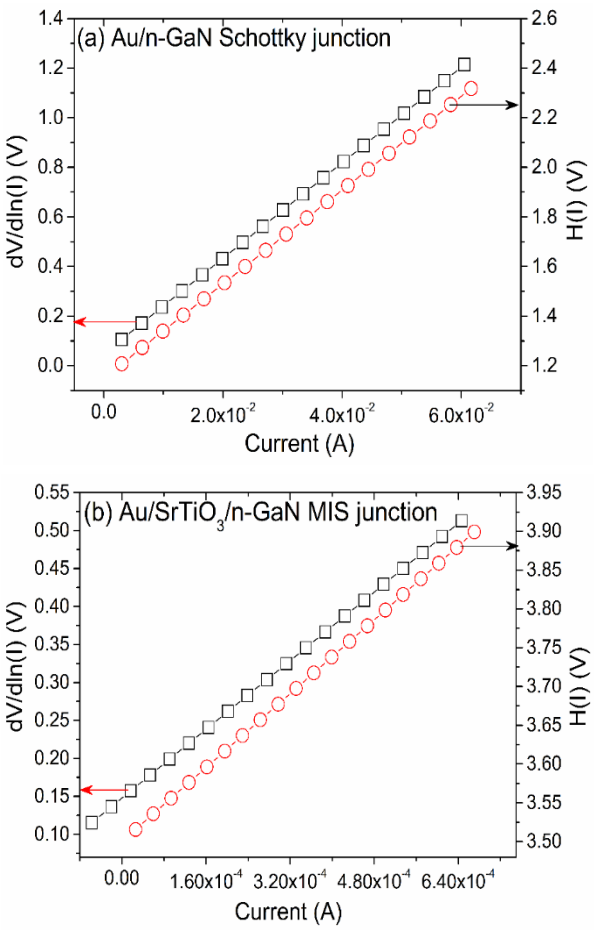

Fig. 3 – Plots of $dV/d(\ln I)$ versus I and $H(I)$ versus I for the (a) Au/*n*-GaN SJ and (b) Au/$SrTiO_3$/*n*-GaN MIS junction

Fig. 4 shows the $1/C^2$–V plot of the Au/*n*-GaN SJ and Au/$SrTiO_3$/*n*-GaN MIS junction measured at a frequency of 1 MHz. Using the Schottky-Mott relationship between C and V, [10], the BHs were determined to be 0.77 and 0.92 eV for the SJ and MIS junction, respectively. The estimated electrical parameters of the SJ and MIS junction by I-V, C-V methods are summarized in Table 1. From Table 1, the BH derived for the MIS junction is more than that of the Au/n-GaN SJ. This may be due to the $SrTiO_3$ layer produced substantial modification in the work function of the metal and in the semiconductor's electron affinity. As a result, the effective BH is altered. Further, both junctions exhibited the BH increase in forward-bias which may be because of the enhancement in quasi-Fermi level of the majority carriers on the GaN surface. Consequently, the majority of the electrons to be inserted directly into the metal that makes a thermionic current via a few electrons are trapped by interface states. As a result, the BH rises thus decreasing the junction current [10]. Moreover, the BH values obtained from the *C-V* approach are larger than those determined from the *I-V* approach for the Au/*n*-GaN SJ and Au/$SrTiO_3$/*n*-GaN MIS junction. This difference in the values of the BHs is achieved from the *I-V* and *C-V* characteristics. This may be due to the spatially inhomogeneous barriers which may be defined by Gaussian distributions of the BHs. These inhomogeneities primarily affect the *I-V* data that probe local electrical properties since the current is obstructed by local patches of low and high BHs and that the current preferentially flows through the lower BH patchy areas resulting in a lower BH, whereas the capacitance of the junction depends only on the average value of the barrier distribution [11, 12].

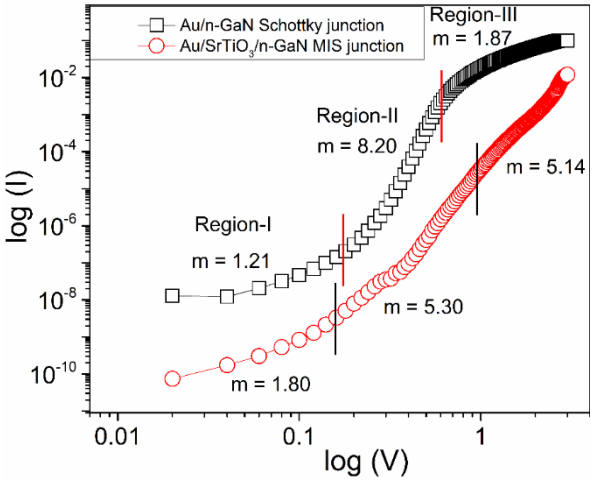

Fig. 4 – Plot of $1/C^2$–V for the Au/*n*-GaN SJ and Au/$SrTiO_3$/*n*-GaN MIS junction

To investigate the current conduction mechanism in the forward bias, a log*V*-log*I* plot is drawn for the Au/*n*-GaN SJ and Au/$SrTiO_3$/n-GaN MIS junction and is illustrated in Fig. 5. The plot exhibits three discrete regions (namely, region I, II, and III) for both SJ and MIS junction that changes the power-law exponent m in the formula $I \alpha V^m$. The value of m is achieved from the slope of linear fit to the log V-log I plot. In region I (Fig. 5), both SJ and MIS junction exhibit the current directly proportional to the applied voltage ($I \alpha V$). This indicates that the current transport follows Ohm's law at low-voltage region, which ruled by the existence of back ground doping and thermally generated carriers are dominant over the injected charge carriers [13]. It is observed in region II, the current raised exponentially for SJ and MIS junction, in which the slope values are greater than 2. This could be associated to the space-charge-limited current (SCLC) employed by a discrete trapping level, where carrier injection is controlled by the presence of injected space charge [14]. Also, it is detected that the slope values of the SJ and MIS junction gradient to decrease at higher voltage region (region-III) as the junctions reached the "trap-filled" limit. As a result, the strong electron injection, electrons escape from the traps and contribute to the space-charge-limited current (SCLS) [15]. Clearly, the observation reveals that a clear variation from an Ohmic-type conduction at lower voltage range (region-I) to a space-charge-limited conduction at higher voltage range (region-II and region-III) for both the SJ and MIS junctions.

Further, in view of Poole-Frenkel emission (PFE) or Schottky emission (SE) mechanisms, the reverse leakage current mechanism is investigated in the Au/*n*-GaN SJ and the Au/$SrTiO_3$/*n*-GaN MIS junction. The theoretical values of PFE and SE field lowering coefficients (β_{PF} and β_{SC}) can be calculated from the equation $2\beta_{SC} = \beta_{PF} = (q3/\pi\varepsilon_o\varepsilon_r)^{1/2}$ [15]. β_{PF} is always twice the

value of the β_{SC}. The derived theoretical values of β_{PF} and β_{SC} obtained for the SJ are 2.46×10^{-5} eVm$^{1/2}$V$^{-1/2}$ and 1.23×10^{-5} eVm$^{1/2}$V$^{-1/2}$, respectively. Similarly, for the MIS junction they are 0.43×10^{-5} eVm$^{1/2}$V$^{-1/2}$ and 0.21×10^{-5} eVm$^{1/2}$V$^{-1/2}$, respectively. A plot of ln(I_R) versus $V_R^{1/2}$ was drawn for the Au/*n*-GaN SJ and Au/SrTiO$_3$/*n*-GaN MIS junction and is illustrated in Fig. 6. The determined experimental slope value is 2.52×10^{-5} eV m$^{1/2}$V$^{-1/2}$ for the Au/*n*-GaN SJ, which agrees well with the theoretical slope of the PFE.

Table 1 – The barrier height, ideality factor, series resistance and shunt resistance of Au/*n*-GaN SJ and Au/SrTiO$_3$/*n*-GaN MIS junction

Parameter	Au/*n*-GaN SJ	Au/SrTiO$_3$/ *n*-GaN MIS
I-V method		
Barrier height (eV)	0.67	0.83
Ideality factor (n)	1.44	1.78
Leakage current (A) at – 1 V	1.8×10^{-6}	9.5×10^{-8}
Series Resistance, *Rs* (Ω)	30	250
Shunt resistance, *Rsh* (Ω)	1.8×10^{6}	2.12×10^{-9}
Cheung's method		
dV/*d*(ln*I*) vs. *I*		
Series resistance (Ω)	19	565
Ideality factor (n)	1.87	4.16
H(*I*) vs. *I*		
Barrier height (eV)	0.61	0.84
Series resistance (Ω)	18	595
C-V method		
Built-in potential (V)	0.75	0.86
Barrier height (eV)	0.77	0.92

Hence, the current conduction mechanism is dominated by PFE in the SJ. However, in the case of MIS junction (Fig. 6), it is detected by two distinct regions, thus indicating that two different conduction mechanisms occur in the reverse bias region. The determined experimental slope values in region I (lower-bias region) and region II (higher-bias region) are 3.94×10^{-5} eVm$^{1/2}$V$^{-1/2}$ and 1.99×10^{-5} eVm$^{1/2}$V$^{-1/2}$, respectively, for the MIS junction. The derived experimental slope value in the lower bias region is nearly matched to the theoretical slope value of the PFE, indicating the PFE is dominant. This may be the occurrence of a high density of structural defects or trap levels in the dielectric film employed here, which could be accountable for the improved performance of the trapping/detrapping of charge carriers [16]. Whereas, the determined experimental slope in the higher bias region is closer to the theoretical slope value of the SE. This indicates that the SE is dominant in the higher bias region where current conduction ensues via the contact interface rather than from the bulk material which attributable to the non-uniformity and subatomic structure of the dielectric layer [17, 18].

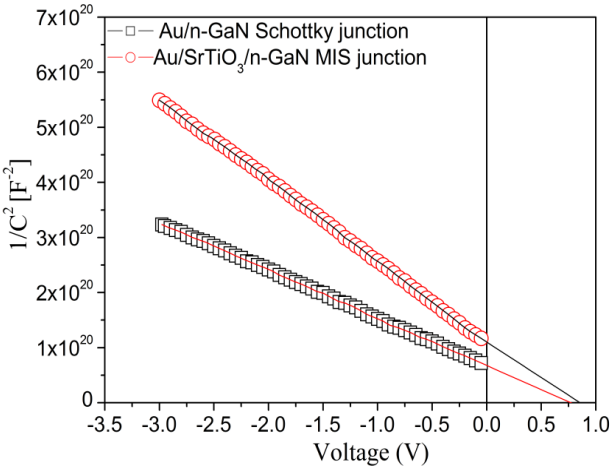

Fig. 5 – Plot of the forward bias log(*I*) vs log(*V*) for Au/*n*-GaN SJ and Au/SrTiO$_3$/*n*-GaN MIS junction

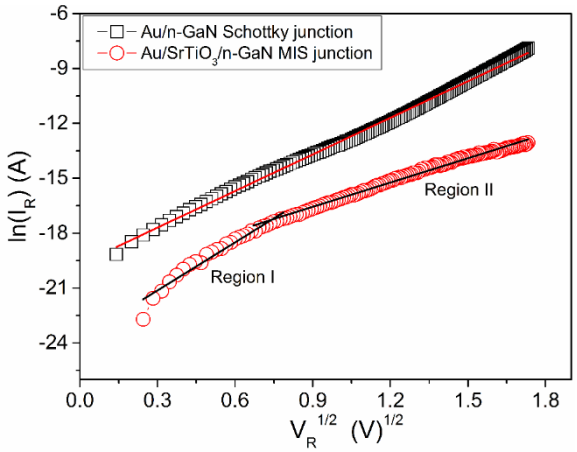

Fig. 6 – Plot of ln(I_R) vs $V_R^{1/2}$ for Au/*n*-GaN SJ and Au/SrTiO$_3$/*n*-GaN MIS junction

4. CONCLUSIONS

The Au/SrTiO$_3$/*n*-GaN MIS junction was fabricated by place of a high-*k* strontium titanate (SrTiO$_3$) in between the Au and *n*-GaN layers, and its electrical properties were explored by *I-V* and *C-V* approaches. The results of MIS junction correlate with the SJ results. The MIS junction revealed a good rectifying nature than the SJ junction. The BH and ideality factor values were determined as 0.67 eV, 1.44 for the SJ junction and 0.83 eV, 1.78 for the MIS junction, respectively. Higher BH was obtained for the MIS junction as compared to the SJ junction. This indicates that the SrTiO$_3$ insulating layer rehabilitated the effective BH. Results indicate the ohmic nature and space-charge-limited conduction at lower and higher voltage regions of forward bias *I-V* characteristic of the SJ and MIS junction. Analysis suggests that the Schottky emission is ruled by the reverse leakage current mechanism in the SJ. Nevertheless, for the MIS junction, the Schottky emission and Poole-Frenkel conduction mechanism were dominant in the lower and higher bias regions, respectively.

REFERENCES

1. H.-S. Kang, M.S.P. Reddy, D.-S. Kim, K.-W. Kim, J.-B. Ha, Y.-S. Lee, H.-C. Choi, J.-H. Lee, *J. Phys. D: Appl. Phys.* **46**, 155101 (2013).
2. T.T.A. Tuan, D.-H. Kuo, *Mater. Sci. Semicond. Proc.* **30**, 314 (2015).
3. K.H. Goh, A.S.M.A. Haseeb, Y.H. Wong, *Thin Solid Films* **606**, 80 (2016).
4. V. Rajagopal Reddy, P.R. Sekhar Reddy, I. Neelakanta Reddy, C-J. Choi, *RSC Adv.* **6**, 105761 (2016).
5. M.T. Danielle, A. Safari, C.K. Lisa, *J. Am. Ceram. Soc.* **79**, 1593 (1996).
6. P. Irvin, J. Levy, R. Guo, A. Bhalla, *Appl. Phys. Lett.* **86**, 042903 (2005),
7. O. Gullu, A. Turut, *Mater. Sci. Pol.* **33**, 593 (2015).
8. O. Gullu, A. Turut, *Microelectron. Eng.* **87**, 2482 (2010).
9. Ashutosh Kumar, M. Heilmann, Michael Latzel, Raman Kapoor, Intu Sharma, M. Gobelt, Silke H. Christiansen, Vikram Kumar, Rajendra Singh, *Sci. Rep.* **6**, 27553 (2016).
10. V. Rajagopal Reddy, V. Janardhanam, Jonghan Won, Chel-Jong Choi, *J. Colloid Interface Sci.* **499**, 180 (2017).
11. P. Prabhu Thapaswini, R. Padma, N. Balaram, B. Bindu, V. Rajagopal Reddy, *Superlattice. Microstruct.* **93**, 82 (2016).
12. C. Venkata Prasad, M. Siva Pratap Reddy, V. Rajagopal Reddy, Chinho Park, *Appl. Sur. Sci.* **427**, 670 (2018).
13. S. Aydogan, U. Incekara, A.R. Deniz, A. Turut, *Microelectron. Eng.* **87**, 2525 (2010).
14. Y.S. Ocak, M. Kulakci, T. Kilicoglu, R. Turan, K. Akkilic, *Synth. Met.* **159**, 1603 (2009).
15. V. Manjunath, V. Rajagopal Reddy, P.R. Sekhar Reddy, V. Janardhanam, Chel-Jong Choi, *Curr. Appl. Phys.* **17**, 980 (2017).
16. A.C. Varghese, C.S. Menon, *Eur. Phys. J. B* **47**, 485 (2005).
17. D.N. Khan, M.H. Sayyad, *Second International Conference on Computer Research and Development, Kualalumpur*, 535 (2012).
18. V. Janardhanam, I. Jyothi, Sung-Nam Lee, V. Rajagopal Reddy, Chel-Jong Choi, *Thin Solid Films* **676**, 125 (2019).

Електричні характеристики переходу Шоткі Au/*n*-GaN з ізоляційним шаром High-*k* $SrTiO_3$

Varra Niteesh Reddy, D.V. Vivekananda, G. Sai Krishna, B. Sri Vivek, P. Vimala†

Department of Electronics & Communication Engineering, Dayananda Sagar College of Engineering, Shavige Malleshwara Hills, Kumaraswamy Layout, Banashankari, Bengaluru-560078 Karnataka, India

Електричні характеристики переходу Шоткі Au/*n*-GaN (SJ) вдосконалювалися з використанням ізолюючого шару високоміцного титанату стронцію ($SrTiO_3$) в середині шарів Au і *n*-GaN. Розглянуто електричні властивості Au/*n*-GaN SJ та Au/$SrTiO_3$/*n*-GaN метал/ізолятор/напівпровідник (MIS) переходу методами струм-напруга і емність-напруга. MIS перехід показав вишуканий випрямляючий характер порівняно з SJ. Встановлено, що послідовний опір та опір шунту становлять 30 Ω, 4.69×10^6 Ω та 250 Ω, 2.12×10^9 Ω, відповідно, для SJ та MIS переходу. Розрахункова висота бар'єру і коефіцієнти ідеальності SJ і MIS переходу становили 0.67 еВ, 1.44 і 0.83 еВ, 1.78, відповідно. Більше значення висоти бар'єру було досягнуто для MIS переходу у порівнянні з SJ, що свідчить про те, що висота бар'єру ефективно змінювалася за допомогою шару $SrTiO_3$. Крім того, коефіцієнт ідеальності, висота бар'єру і послідовний опір SJ і MIS переходу оцінювалися за допомогою функції Ченга і порівнювалися між собою. Спостереження показують омічну поведінку в областях з низькою напругою і провідність, обмежену об'ємним зарядом, в областях з вищою напругою у прямому зсуві *I-V* характеристики для SJ і MIS переходу. Крім того, досліджено механізм провідності зворотного струму витоку SJ і MIS переходу.

Ключові слова: GaN *n*-типу, Титанат стронцію, Електричні властивості, MIS перехід, Висота бар'єру, Коефіцієнт ідеальності, Механізм провідності струму.